Received: 3 October 2019 | Revised: 16 April 2020 | Accepted: 17 April 2020

DOI: 10.1002/cyto.b.21882

ORIGINAL ARTICLE

CLINICAL CYTOMETRY WILEY

Single-cell profiling of pediatric T-cell acute lymphoblastic leukemia: Impact of *PTEN* exon 7 mutation on PI3K/Akt and JAK–STAT signaling pathways

Paola Bonaccorso[1,2] | Cristina Bugarin[1] | Chiara Buracchi[1] | Grazia Fazio[1] | Andrea Biondi[1,3] | Luca Lo Nigro[2] | Giuseppe Gaipa[1]

[1]M. Tettamanti Research Center , University of Milano-Bicocca, San Gerardo Hospital, Monza, Italy

[2]Center of Pediatric Hematology Oncology, Azienda Policlinico-OVE, University of Catania, Catania, Italy

[3]Pediatric Clinic, University of Milano Bicocca, Fondazione MBBM/Ospedale San Gerardo, Monza, Italy

Correspondence
Luca Lo Nigro, Head of Cytogenetic, Cytofluorimetric and Molecular Biology Lab Azienda Policlinico – OVE University of Catania, Via Santa Sofia 78, 95213, Catania, Italy.
Email: lucalonigro1968@gmail.com, lonigro@policlinico.unict.it

Funding information
Associazione Italiana per la Ricerca sul Cancro, Grant/Award Numbers: AIRC 5x1000 Ref. 21147 (AB) - , AIRC IG 2017 (AB) - , MFAG-2009(LLN); Fondazione Alessandro Maria Zancan ONLUS "GrandeAle ONLUS"; Fondazione M. Tettamanti De Marchi; TRANSCAN-2 Fondazione Regionale per la Ricerca Biomedica

Abstract

Background: The PI3K/Akt/mTOR (PI3K) signaling pathway has a crucial role in T-cell acute lymphoblastic leukemias (T-ALLs). Although loss-of-function of phosphatase and tensin homolog (PTEN) is a common event in pediatric T-ALLs, the exact role of this tumor suppressor in T-ALL development has yet to be defined.

Methods: Here, we report an optimized cytometric method for accurate proteomic profiling of T-ALL leukemic blasts at single-cell level. We determined the expression of PI3K and JAK–STAT signaling components in both primary and immortalized T-ALL cells as well as in normal T cells.

Results: We observed that *PTEN* exon 7 mutated T-ALL cells retain a distinct PI3K activation; in particular, these cells show higher pAkt levels and a lower pS6 expression. Interestingly, we demonstrated for the first time that *PTEN* exon 7 mutated T-ALL are nonresponsive to IL7 in vitro as assessed by lack of pSTAT5 activation, although they do express IL7R.

Conclusions: Phosphoflow analysis represents a fast, reliable, and accurate method to study the signaling profile of T-ALL. *PTEN* exon 7 mutated T-ALL cells are nonresponsive to IL7 in vitro suggesting that they may activate other mechanisms to support their viability and proliferation such as a higher constitutive PI3K/Akt signaling. Further investigations are necessary to elucidate the significance of this peculiar signaling behavior. Our observations should be taken into account in future studies aiming at molecular targeting of PI3K and/or JAK/STAT pathways for pharmacological intervention in T-ALL.

KEYWORDS
acute lymphoblastic leukemia, cell signaling, childhood, interleukin 7, phoshoflow, PTEN

1 | INTRODUCTION

T-lineage acute lymphoblastic leukemia (T-ALL) is an aggressive hematologic cancer that accounts for about 15% of pediatric and 25% of adult ALL cases (Hunger & Mullighan, 2015; Litzow & Ferrando, 2015). In the last few years, enormous progress was made in T-ALL genetics and biology understanding, but there are still significant gaps in our knowledge. The recent identification of mutations and chromosomal abnormalities have provided an additional view on the genetic T-ALL subgroups characterized by deregulation of various cellular processes (Belver & Ferrando, 2016; Bongiovanni, Saccomani, & Piovan, 2017; Girardi, Vicente, Cools, & De Keersmaecker, 2017; Liu et al., 2017).

Paola Bonaccorso and Cristina Bugarin contributed equally to this study.

PI3K/Akt is a major signaling pathway implicated in T-ALL malignant transformation promoting several functions including cell survival and proliferation (Okkenhaug & Vanhaesebroeck, 2003). The major negative regulator of this pathway is the tumor suppressor lipid phosphatase and tensin homolog (PTEN), a lipid phosphatase that dephosphorylates PIP3 into PIP2, which is frequently inactivated in human cancer (Chow & Baker, 2006; Mendes, Cante-Barrett, Pieters, & Meijerink, 2016; Milella et al., 2015). Constitutive hyperactivation of the PI3K/Akt pathway is a very common event in T-ALL that is involved in sustaining leukemic cell viability and maintenance, and there is evidence that it can be aberrantly activated by cell-autonomous lesions (Oliveira et al., 2017; Sakai, Thieblemont, Wellmann, Jaffe, & Raffeld, 1998; Shan et al., 2000). *PTEN*non-sense or frame-shift mutations cluster in exon 7, resulting in a C-terminal truncated protein, rapidly degraded and thus leading to a decreased or absent *PTEN* protein expression and activity (Georgescu, Kirsch, Akagi, Shishido, & Hanafusa, 1999; Sansal & Sellers, 2004; Zuurbier et al., 2012). The prognostic significance of *PTEN* inactivation and PI3K/AKT aberrant activation is still unclear (Jenkinson et al., 2016; Jotta et al., 2010; Paganin et al., 2018). *PTEN* mutations, resulting in loss of *PTEN* protein, were reported in 17% of T-ALLs (Palomero et al., 2007). Furthermore, more than 85% of T-ALLs have been shown to display hyperactivated signaling due to post-translational inactivation of *PTEN* by casein kinase 2 (CK2)-mediated phosphorylation and/or oxidation by reactive oxygen species (Silva et al., 2008; Zuurbier et al., 2012). The majority of *PTEN* alterations occur at the level of exon 7, and are caused by small insertion/deletions that lead to truncation of the protein due to premature termination of translation (Gutierrez et al., 2009; Zuurbier et al., 2012).

Interleukin 7 (IL7) promotes cell survival and cell cycle progression during normal T-cell development (Barata et al., 2004; Johnson, Shah, Bajer, & LeBien, 2008). Upon ligand binding, the IL7 receptor (IL7R) dimerizes and induces the phosphorylation of JAK3 and JAK1 (Silva et al., 2011). Activated JAKs allow the recruitment and phosphorylation of signal transducer and activator of transcription 5 (STAT5), which in turn can regulate the transcription of target genes such as B-cell CLL/lymphoma2 (Bcl-2) family members (Jiang et al., 2005). It has been recently demonstrated that IL7-mediated upregulation of *BCL2* in T-ALL is independent of STAT5 activity, suggesting that STAT5 could promote the viability of malignant T cells by alternative Bcl-2 independent mechanisms. Moreover, it has been showed that STAT5 directly downregulates *BCL6* and promotes the expression of PIM1 in response to IL7 stimulation (Ribeiro et al., 2018).

IL7/IL7R pathway can promote leukemogenesis in vivo (Abraham et al., 2005; Rich, Campos-Torres, Tepper, Moreadith, & Leder, 1993), or can drive disease progression by regulating cell viability and proliferation (Dibirdik et al., 1991; Silva et al., 2011).

Although western blotting (WB) is the gold standard technique to study the proteomic profile of hematological malignancies, phosphoflow cytometry has been shown to provide several advantages over WB such as real-time measurement of multiple and simultaneous events in single cells (Tazzari et al., 2002), as well as the characterization of rare subsets of cells even within heterogeneous samples (Krutzik, Irish, Nolan, & Perez, 2004).

In this study, we have characterized PI3K/Akt/mTOR (PI3K) and JAK–STAT pathways at single cell level within a cohort of pediatric T-ALL patients by carrying out phosphoflow cytometry. The results reported herein show that *PTEN* exon 7 mutated T-ALL display a distinct signaling pathway and that phosphoflow approach is a feasible and robust tool for accurate investigation of this subset of T-ALL patients including in vitro screening of targeted inhibition molecules.

2 | PATIENTS AND METHODS

2.1 | Primary pediatric samples

Bone marrow (BM) or peripheral blood-derived leukemic cells were collected from 25 children with T-ALL enrolled in the AIEOP ALL 2009 or R2006 protocols at the Pediatric Clinic of University Milano Bicocca, at San Gerardo Hospital. Mononuclear cells were collected by Ficoll-Paque centrifugation, washed twice in culture medium (RPMI-1640 supplemented with 10% fetal bovine serum [FBS]), and then cryopreserved in RPMI-1640 with 10% DMSO. All specimens consisted of 85–100% of blasts. Features of these patients are summarized in Supplemental Table S1. Moreover, we collected 11 BM control samples from patients without hematological diseases.

2.2 | Cell cultures

CEM, Jurkat, and HPB-ALLT-ALL cell lines were cultured in RPMI-1640 medium supplemented with 10–20% FBS, 100 IU/ml penicillin, 100 μg/ml streptomycin, and 1% L-glutamine, at 37°C in humidified air containing 5% CO_2. 293T cell line (cultured in Dulbecco's modified Eagle medium high glucose with 10% FBS) and CEM were used respectively as positive and negative control for PTEN comparative detection in WB and phosphoflow analysis. Cell survival experiments with either primary T-ALL samples or Jurkat cells are described in more detail in Supplemental Information, briefly cells were cultured in RPMI-1640 medium supplemented with 5% FBS and 25 ng/ml of recombinant human IL7 (Peprotech) and cell viability was determined at 72 hr using annexin V-7AAD apoptosis kit and the manufacturers' instructions (R&D System).

2.3 | Flow cytometry (FC) immunophenotyping

Immunophenotyping at diagnosis was performed by standard multiparametric FC on fresh samples processed within 24 hr from collection. The diagnosis of T-ALL was based on standard criteria. Briefly, whole blood nucleated cells were incubated with a cocktail of conjugated monoclonal antibodies (MoAbs) for 15 minutes at room temperature and 30,000 total events for each tube were acquired on a FACScanto II™ flow cytometer (Becton Dickinson) and analyzed with Diva software (Becton Dickinson). A summary of the diagnostic immunophenotyping performed in the studied patients is reported in Supplemental Table S2.

2.4 | Phosphoflow cytometry

Thawed mononuclear cells from primary T-ALL samples were assessed for count and viability with trypan blue die before phosphoflow testing. Fresh cell lines or primary thawed cells were starved in X-VIVO medium and rested at 37°C for 16 hr or 1 hr, respectively, thereafter cells viability was checked again, and only samples with ≥70% of viability were used for phosphoflow experiments. Then, cells were stimulated with IL7 (50 ng/ml) or inhibited with NVP-BEZ 235 (800 nM) and incubate 15 or 30 minutes at 37°C, respectively. Cells were then fixed with 1.5% paraformaldehyde and permeabilized with 90% ice-cold methanol prior to staining with anti-phospho-protein-directed MoAbs (or isotype matched IgG) and surface antigen-directed MoAbs anti CD7 ECD (Beckman Coulter) and anti-CD45 PerCP (BD). Characteristics of MoAbs are described in Supplemental Table S3.

Cells were acquired on a FACSaria flow cytometer (BD) equipped with 488-, 633-, and 405-nm lasers. Data (at least 100,000 events per tube) were collected and analyzed as previously described (Gaipa et al., 2009) using the DIVA software (BD). Primary T-ALL samples that did not reach at least 25% of IL7-inducible pSTAT5 response in residual T cell were excluded from subsequent analyses.

Histogram overlays were carried out by FlowJo Software. Leukemic cells and normal residual T cells were identified by using CD7-ECD and CD45-PerCP antibodies as shown in Supplemental Figure S1a,b.

Positivity threshold for phosphoprotein expression was established by the comparative use of isotype IgG instead of the phosphoprotein specific antibody (Supplemental Figure S1c). Basal level of each phosphoprotein was then calculated as percentage (%) of phosphoprotein positive (p-positive) cells in unstimulated conditions. Response to each cytokine was calculated as percentage of p-positive cells after exposure to cytokine *minus* the percentage of p-positive cells in the basal state. IL7 inducible pSTAT5 signaling in residual normal T cells contained within the primary leukemia samples was considered as positive control of functional signaling. Phosphoprotein expression was also assessed as mean fluorescence intensity (MFI) of the fluorescence distribution in parallel with the % of positive cells.

2.5 | Western blotting

Cells were thawed and collected by centrifugation, washed twice in ice-cold phosphate buffered saline, and pellets were lysed for 30 min at 4°C in RIPA-buffer (Tris–HCl pH 7.4 20 mM, NaCl 20 mM, EDTA pH 8 2 mM, Na_3VO_4 0.2 mM, Triton 1%, NaF 25 mM, β-glycerolphosphate 25 mM), with protease inhibitor cocktail supplemented with 1 mM phenylmethylsulfonyl fluoride to inhibit phosphoproteins. Homogenates were centrifuged 14,000*g* for 10 min 4°C and supernatants were stored at −80°C. Protein concentration was determined with Bradford protein Assay (Sigma-Aldrich, St. Louis, MO). Twenty micrograms of proteins were resolved on an Any kD precast polyacrylamide gel and transferred onto polyvinylidene difluoride membranes. Nonspecific binding sites were blocked by incubation in blocking buffer, 1X tris buffered saline (TBS) containing 0.1% tween-20(TBS/T) and supplemented with 10% bovine serum albumin (BSA) for 2 hr at room temperature. After three TBS/T washes, membranes were incubated with primary antibodies overnight at 4°C in TBS/T with 5% BSA. Then, membranes were washed and incubated with peroxidase conjugate secondary antibodies diluted in TBS/T for 1 hr at room temperature. A StripAblot Stripping Buffer (Euroclone S.p.A., Pero, Italy) was used to recover membranes. Antigens were revealed using Clarity Western Luminol/Enhancer solution and peroxide solution (Clarity Western ECL Substrate BIO-RAD) by Alliance Instrument (Uvitec Software). Densitometry analyses were performed using Uviband Software (Uvitec, Cambridge, UK). The following antibodies were used: rabbit anti-PTEN antibody used at working dilution 1:1,000 (Cell Signaling Technology) and rabbit anti-beta Actin (D6A8) antibody at 1:1,000 (Cell Signaling Technology) to evaluate the quality of protein extracts and goat anti-Rabbit IgG (H+L) (human IgG absorbed); horseradish peroxidase conjugate (BIO-RAD) used at 1:3,000. Positivity or negativity was established by assessing the presence or absence of protein bands.

2.6 | Patients' DNA samples

Genomic DNA samples were collected from primary T-ALLs samples. Sequencing of PTEN exon 7 was performed by PCR amplification, and PCR products were directly sequenced in both directions using Applied Biosystems ABI PRISM-3130 Genetic Analyzer instrument (Life Technologies). Alignment was carried out using the Basic Local Alignment Search Tool database (BLAST, www.blast.ncbi.nlm.nih.gov). Genomic DNA samples were screened for the Type 1 and Type 2 TAL1 deletions by PCR amplification using BIOMED-1 primer sets and PCR conditions (Pongers-Willemse et al., 1999).

2.7 | Reverse transcription quantitative polymerase chain reaction (RT-qPCR)

RNA was extracted from at least 1×10^6 cells using TRIzol (Life Technologies). Total RNA was reverse-transcribed using Superscript II reverse transcriptase and random hexamers, according to the manufacturer's instructions (Invitrogen). Appropriate primers and cDNA were mixed with SYBR Green master mix (Applied Biosystems) and reactions were performed in triplicates in QuantStudio7 Flex (Applied Biosystem). Primers' sequences are described in Supplemental Table S4. Relative expression of the mRNAs was estimated using the ddCt method and the expression levels were normalized by *GUS* as internal control.

2.8 | Statistical analysis

Statistical analyses, as defined in each figure legend, were performed using Prism V6.0 (GraphPad, La Jolla, CA). The *t* test was used to compare the continuous variables relative to proteins and phosphoproteins

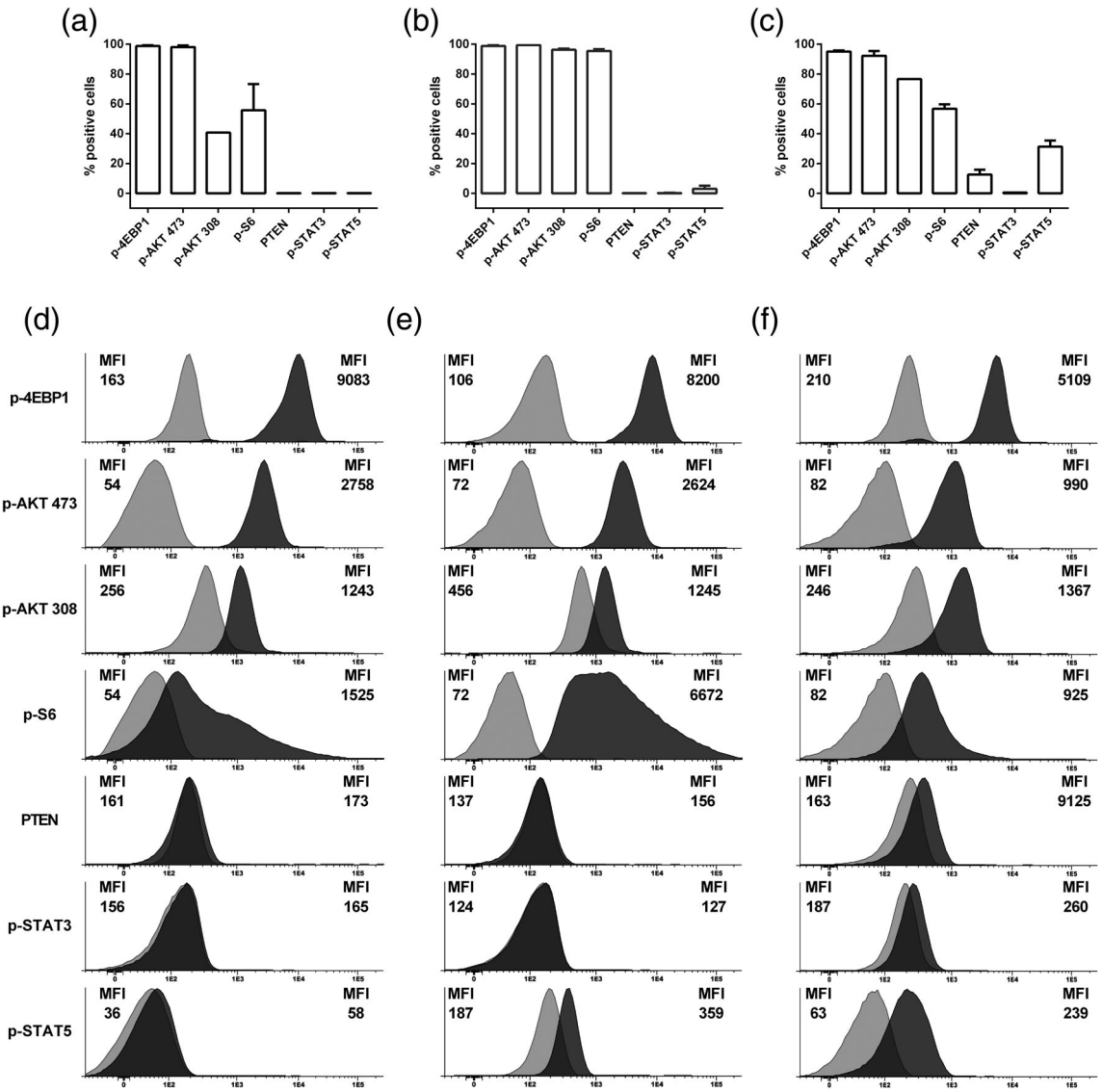

FIGURE 1 Constitutive PI3K and JAK/STAT signaling in T-ALL cell lines with different status of *PTEN*. Basal expression measured by phosphoflow in three T-ALL cell lines representative of different status of *PTEN* gene, percentages are indicated in boxplots and MFI in histograms: CEM (a,d), JURKAT (b,e), and HPB-ALL(c,f). PTEN protein was not expressed neither in CEM nor in JURKAT cells due to their *PTEN* exon 7 mutation, whereas it is expressed in *PTEN* wt HPB-ALL cells. A constitutive hyperactivation of p4EBP1, pAkt473, pAkt308, and pS6 phosphoproteins is observed in all cell lines. JAK/ STAT basal pathway is generally not activated with the exception of HPB-ALL cell line with partial pSTAT5 expression

expression levels as assessed by FC and by phosphoflow. A *p*-value of .05 was used as the cutoff below which results were considered statistically significant.

3 | RESULTS

3.1 | PI3K and JAK/STAT basal signaling in T-ALL cell lines

We first performed a basal level phosphoflow assay in CEM, Jurkat, and HPB-ALL cell lines carrying different *PTEN* status. After starvation in X vivo medium, the mean cell viability observed for all experiments was >90%. We observed a constitutive hyperactivation of the PI3K pathway in all the analyzed cell lines. Moreover, we assessed the basal level of phosphorylated JAK/STAT downstream targets and found elevated levels of pSTAT5 only in HPB-ALL cell line (31.3 ± 4.1%), whereas pSTAT3 was inactive in all tested cell lines. PTEN protein expression was detected in HPB-ALL*PTEN*wild-type (wt) cell line (56.8 ± 3.0%), whereas it was not expressed neither in CEM nor in Jurkat cells due to their *PTEN* genetic mutation (Figure 1a–c). MFI was also evaluated as shown in Figure 1d–f. To determine PTEN expression levels, we carried out phosphoflow and WB analyses in parallel experiments using CEM and 293T cells as negative and positive control respectively. As shown in Supplemental Figure S2, regardless of the method

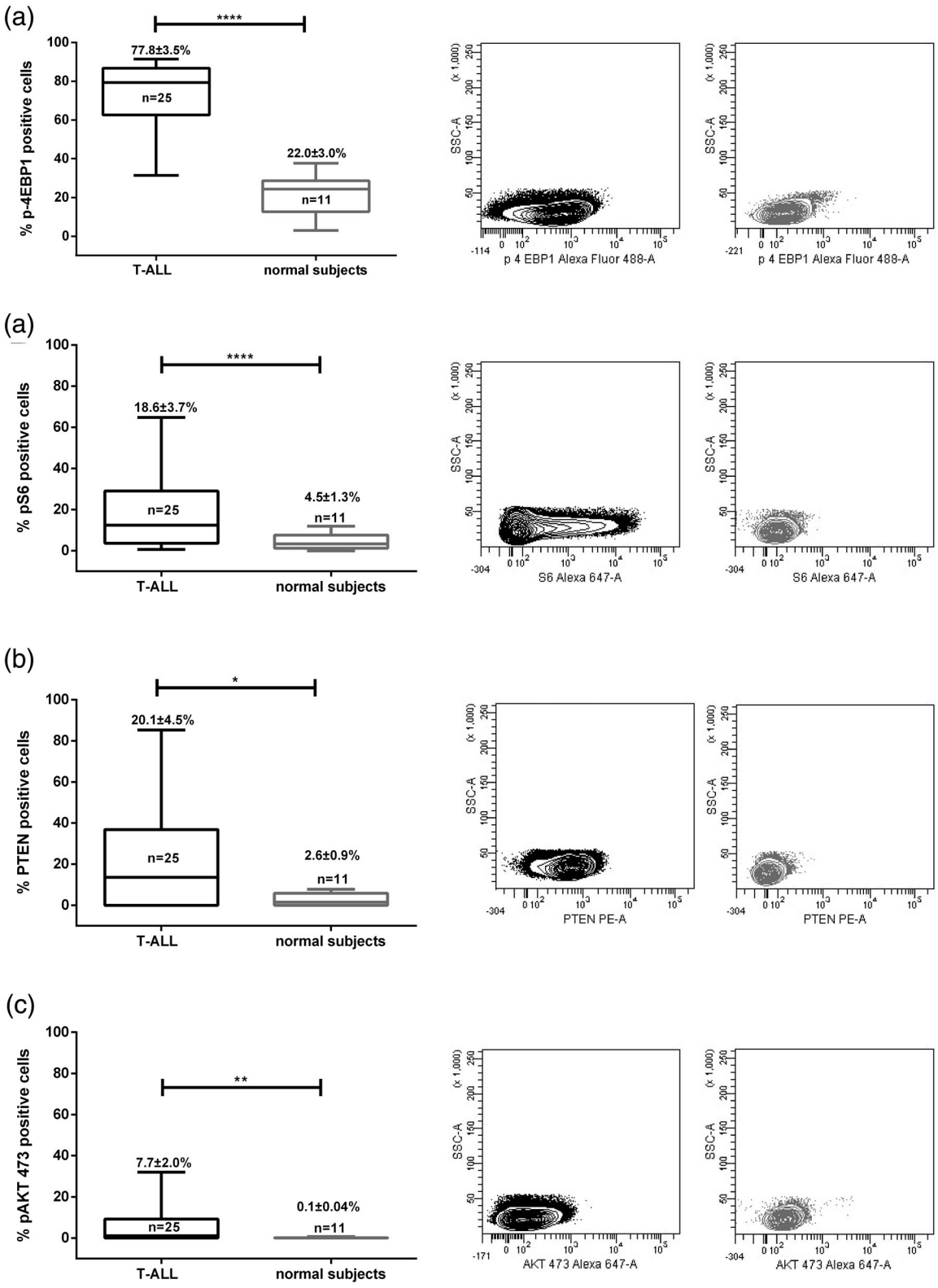

FIGURE 2 PI3K constitutive signaling in primary T-ALL cells. Primary T-ALL blasts show constitutive hyperactivation of the PI3K pathway as compared to T cells from normal BM samples. Expression of % p4EBP1, pS6, PTEN, and pAkt473 proteins and respective representative contour plot are reported in Graphs (a–d)

employed, 293T cells tested positive for PTEN expression, whereas CEM cells were PTEN negative.

3.2 | PI3K basal signaling in primary T-ALL samples according to PTEN mutation

We next sought to determine basal expression level of the PI3K signaling in blasts from 25 primary T-ALL samples and in T cells from 11 normal BM samples. Cell viability of thawed primary cells after starvation in X vivo medium was 85.2% *SD* = 8.0%, range 70–95%. Two samples were excluded from the phosphosignaling analyses because they did not meet the predetermined criterion of either ≥70% of viable cells or at least 25% of IL7-inducible pSTAT5 response in residual T cell within the T-ALL samples. In this regard, samples included in the final analyses showed a mean pSTAT5 response of 48.9% (*SD* = 10.5, range 26.4–64.3%).

Similarly to cell lines, we found constitutive hyperactivation of the PI3K downstream targets in most of samples (Figure 2). Specifically, we observed that p4EBP1, pS6, pAkt473, and PTEN were all significantly activated as compared to normal BM samples: (77.8 ± 3.5 vs. 22.0 ± 3.0%, $p < .0001$), (18.6 ± 3.7 vs. 4.5 ± 1.3%, $p < .05$), (7.7 ± 2.0 vs. 0.1 ± 0.04%, $p < .01$), and (20.1 ± 4.5 vs. 2.6 ± 0.9%, $p < .05$), respectively. When we analyzed such molecules according to the *PTEN* status, we noticed that both p4EBP1 and pS6 were more highly expressed in wt patients as compared to *PTEN* mutated cases,

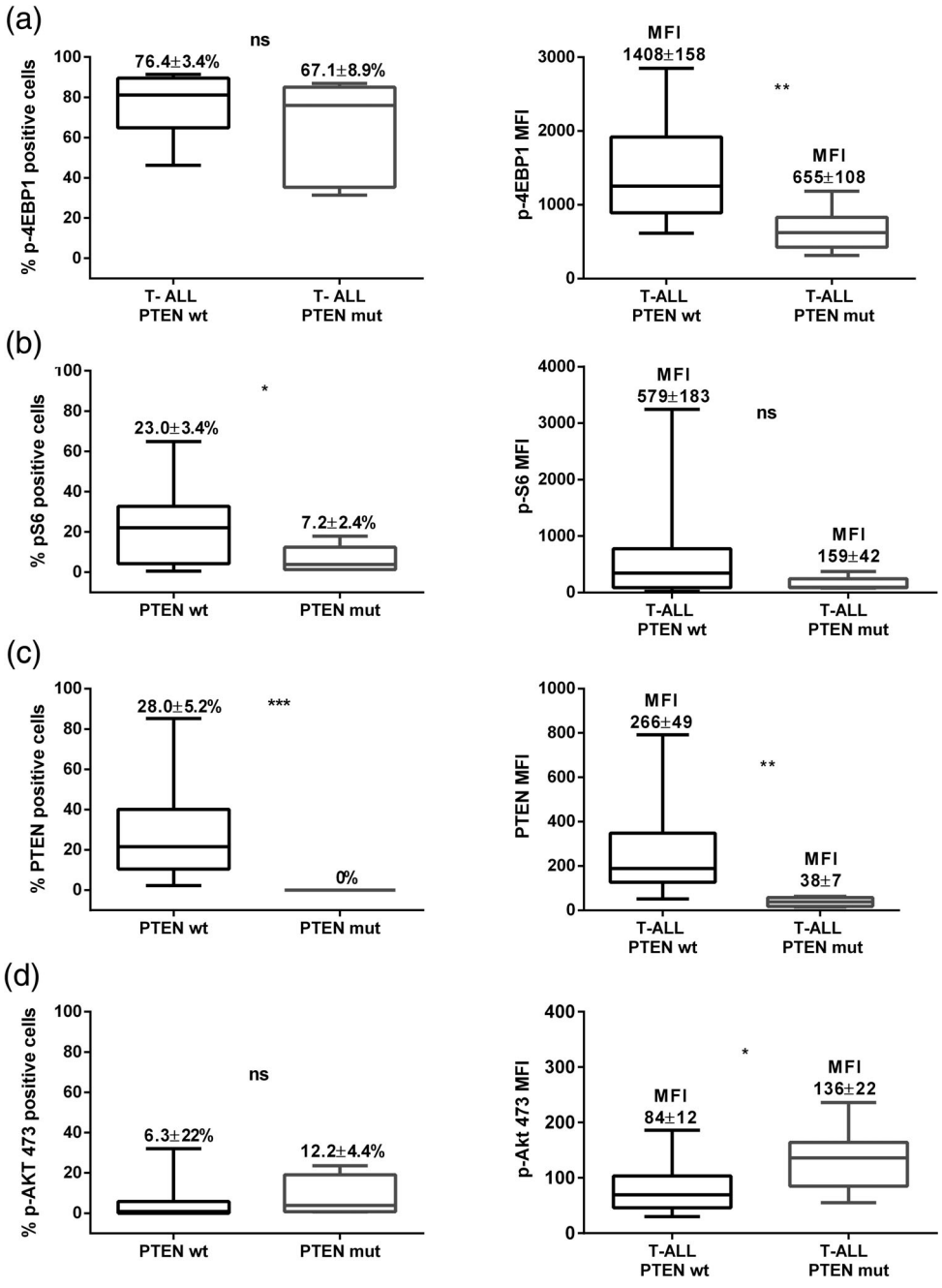

FIGURE 3 PI3K constitutive signaling in primary T-ALL cells according to PTEN status. Basal expression levels of p4EBP1, pS6, PTEN, and pAkt473 proteins was measured in T-ALL patients according to *PTEN* status and are reported as both percentages (Graphs a–d) and MFI values (Graphs e–h). pAkt S473 was more hyper activated in PTEN mutated samples although this difference was significative only by MFI. By contrast, pS6 and p4EBP1 were under expressed in PTEN mutated although these differences are not consistent if measured as % or as MFI. As expected, *PTEN*-mutated T-ALL samples did not express PTEN protein

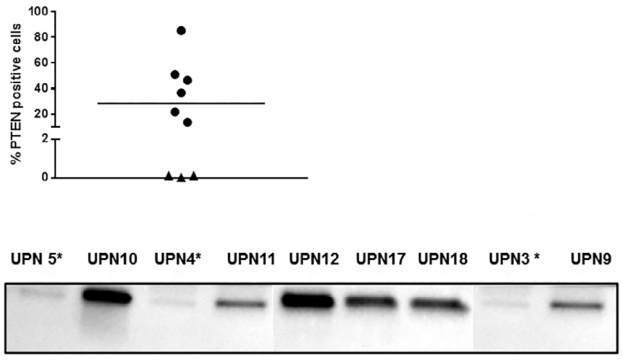

FIGURE 4 Analysis of PTEN expression according to genetic lesion. PTEN protein expression in *PTEN* exon 7 wt (n = 6) and in *PTEN* exon 7 mutated (n = 3) T-ALL patients, as assessed by phosphoflow (a) and WB (b). Panel (a) shows the % of PTEN-positive cells by phosphoflow. *PTEN* exon 7 wt and mutated patients are indicated by circles and triangles respectively. Panel (b) shows the WB analysis: protein bands of each patient are indicated by the individual UPN codes of *PTEN* wt and mutated (*) patients

but these differences were significant only if measured as % or MFI, respectively. (Figure 3, Panels a,e and Panels b,f). As expected, *PTEN* mutated T-ALL samples did not express PTEN protein (Figure 3c,g). pAkt S473 was more hyper activated in PTEN mutated samples although this difference was significative only by MFI (Figure 3d,h). Normal residual T cells were detectable in 19 out of 25 T-ALL samples, and indeed they reproduced the signaling pattern observed in T cells derived from normal BM, confirming their reliable use as internal control for comparative phosphoflow analyses. In this regard measurements as % of positive cells or as MFI provided very similar results (Supplemental Figure S3).

Furthermore, we measured PTEN expression using both WB and phosphoflow in parallel on nine primary T-ALL samples (six *PTEN* wt and three *PTEN* exon 7 mutated); we obtained concordant results confirming that phosphoflow is a reliable and accurate approach to measure PTEN expression in T-ALL (Figure 4).

3.3 | PI3K signaling inhibition and IL7-induced JAK/STAT pathway activation according to PTEN status

To measure changes in the basal signaling pathways, we used either the dual inhibitor of PI3K pathway NVP-BEZ235 or IL7. As shown in Figure 5, we observed an inhibition of p4EBP1, pAkt, and pS6 phosphorylation in primary T-ALL samples regardless of *PTEN* status. We then assessed the basal phosphorylation levels of STAT5 in 23 T-ALL primary samples (16 *PTEN* wt and 7 *PTEN* exon 7 mutated) as well as in their normal residual T-cell compartment. Basal pSTAT5 signal was generally low in both the subgroups (6.3 ± 3.5 vs. 0.07.x ± 0.03%, p = ns as well as in normal residual T cells (0.1 ± 0.09%), (Figure 6a, dark bars). Exceptions were observed in three patients (all *PTEN* wt): UPN15 carrying NUP214/ABL1 fusion gene (pSTAT5 = 43.3%), UPN17 carrying ETV6/ABL1 (pSTAT5 = 33.6%), and UPN24 IL7R mutated (pSTAT5 = 23.3%). Interestingly, when we assessed IL7-induced pSTAT5 response, all 16 *PTEN* wt T-ALL blasts significantly increased their pSTAT5 expression as compared to basal level (mean = 47.3 ± 5.3%, p < .001) similarly to the strong response of normal residual T cells (mean = 49.4 ± 2.4%, p < .001); by contrast, all the *PTEN* exon 7 mutated samples showed a lack or very low pSTAT5 (mean = 6.2 ± 2.3%, p not-significative, Figure 6a, gray bars). This observation was confirmed by measuring MFI of pSTAT5 expressing cells (Figure 6b). Regarding cell lines, only *PTEN* wt HPB-ALL cells (mean basal level = 28.3 ± 6.9%) was able to activate pSTAT5 upon IL7 stimulation (mean = 92.4 ± 2.8%), while *PTEN* deleted or mutated CEM and Jurkat cells were completely nonresponsive (mean pSTAT5 = 0.1 and 3.2%, respectively; Figure 6c), and assessment by measuring MFI gave similar results (Figure 6d).

Regarding IL7-induced PI3K signaling response, we studied the p4EBP1, pS6, and pAkt components in six T-ALL samples (three T-ALL *PTEN* wt and three *PTEN* mutated samples) including normal residual T cells in the analysis. We did not observe any significative activation neither in T-ALL nor in T lymphocytes activation (Supplemental Figure S4), indicating that such pathways might not be directly activated by IL7.

To investigate the lack of pSTAT5 response in *PTEN* mutated T-ALL cells, we measured CD127 and CD132 (both of IL7 receptor components) surface expression in T-ALL blasts from 18 patients (7/18 *PTEN* exon 7 mutated and 11/18 *PTEN* wt). As shown in Figure 7a, we found that the expression of IL7 receptor (IL7 R) proteins was clearly detectable in all *PTEN* exon 7 mutated samples despite they were pSTAT5 nonresponsive; however, CD127 was statistically lower as compared to wt samples (CD127: mean 19.4 ± 3.8 vs. 57.7 ± 7.9%, p < .01; CD132: mean 46.7 ± 11.7 vs. 59.9 ± 8.0%). Regarding CD127 expression, we aimed at investigating the correlation between its surface expression and the IL7-induced pSTAT5 response, by a regression plot analysis, and we observed a significative correlation between these parameters (r square = 0.319, p = .01; Figure 7b). Furthermore, we assessed IL7R expression and pSTAT5 response in Jurkat and HPB-ALL cell lines. Jurkat cells expressed both CD127 and CD132 at high levels (65.4 and 84.2%, respectively) despite being pSTAT5 nonresponsive to IL7. Yet, *PTEN* wt HPB-ALL cells showed a very high IL7R expression (CD127 = 97.5% and CD132 = 95.8%), and a strong IL7-induced pSTAT5 response (92.4%). Representative experiments are reported in Figure 7c.

3.4 | IL7-mediated T-ALL cell survival

To explore the functional involvement of IL7-mediated cell growth, we cultured eight primary samples (four *PTEN* exon 7 mutated and four *PTEN* wt) for 72 hr in the presence or absence of IL7. We found that cell survival was not affected in three out of four mutated samples and Jurkat cells showed similar IL7-indipendent survival. In *PTEN* wt samples, the result was heterogeneous with two samples showing an IL7-induced increased survival and two samples not affected (Supplemental Material).

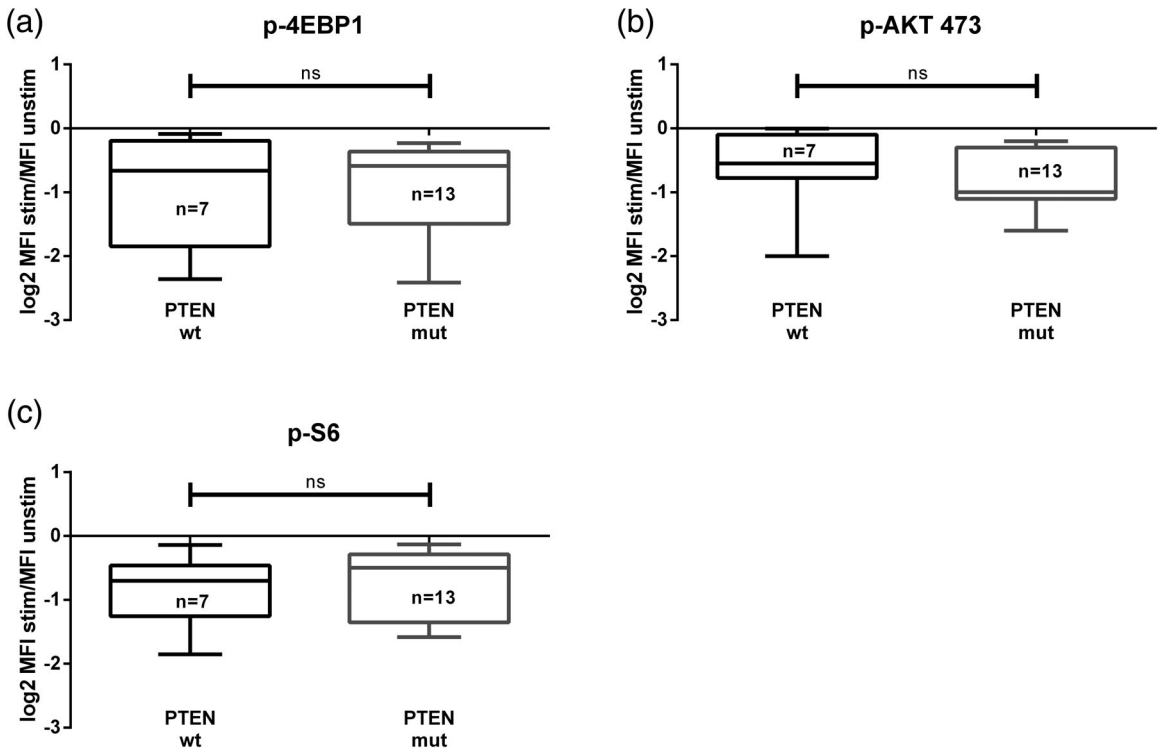

FIGURE 5 BEZ 235-induced inhibition of PI3K/AKT pathway. BEZ inducible PI3K/Akt signaling was measured in both primary T-ALL*PTEN* exon 7 mutated and wt cells. Values are expressed as mean values of MFI log_2 ratio (inhibited/basal state) for p4EBP1 (a), pAkt473 (b), and pS6 (c). BEZ abrogates phosphorylation below basal levels regardless of *PTEN* status

3.5 | RT-qPCR analysis of gene transcript levels IL7 regulated in T-ALL patients

To determine the functional role of IL7 in survival, growth, and proliferation, we also determined the transcription levels of the following genes *PIM1*, *BCL2*, *BCL6*, and *BCL2L1* genes. We studied 19 out of 25 T-ALLs including 5 *PTEN* exon 7 mutated patients. We observed a significantly higher *PIM1* expression in *PTEN* exon 7 wt patients as compared to the mutated ones (p = .032). When we excluded three patients with *PTEN* exon 7 wt and basal pSTAT5 overexpressed (due to mutations in IL7Rα Exon6 and other rearrangements), *PIM1* loses the statistical significance despite the difference in fold change (1.293 vs. 0.588, respectively; Figure 8a). *BCL2* expression was statistically higher in *PTEN* wt patients (Figure 8b), these data support the report by Ribeiro et al. (2018) showing that IL7 upregulates Bcl-2 via PI3K/Akt pathway, therefore in *PTEN* exon 7 mutated T-ALLs STAT5 may induce cell survival by an alternative Bcl-2 independent mechanism. Finally, *BCL6* and *BCL2L1* expression resulted nonstatistically significant between the two subgroups (p > .05; Figure 8c,d).

4 | DISCUSSION

Previous reports demonstrated a cross-talk between IL7R signaling pathway and PI3K that ultimately leads to either STAT5 or Akt activation (Barata et al., 2004). Yet, stimulation by IL7 triggers the phosphorylation of various pathways such as JAK/STAT, Ras/MAPK and PI3K (Barata, Cardoso, & Boussiotis, 2005; Carrette & Surh, 2012). To better understand the role of these signaling pathways in *PTEN*-mutated pediatric T-ALL, we first sought to establish the expression levels of the various PI3K and JAK/STAT downstream effectors using phosphoflow analysis (Krutzik et al., 2004). In our hands, phosphoflow and WB approaches provided consistent results throughout different sets of experiments. Precisely, phosphoflow analysis can be performed in around 3 hr from sample collection or thawing. Reproducibility was high as demonstrated by the consistent signaling profile of normal T lymphocytes detected in both healthy BM samples and in T-ALL samples. Notably this approach can allow to analyze signaling pathways in heterogeneous populations by appropriated gating strategies. In this regard, we were able to dissect different signaling pathways in two different PTEN subclones of the same T-ALL sample (data not shown, manuscript in preparation).

Then, we studied PI3K/Akt pathway in three T-ALL cell lines bearing different *PTEN* status, and we found constitutive hyperactivation of PI3K/Akt pathway in all tested cells confirming previous data (Gusscott et al., 2016; Shan et al., 2000). PTEN protein resulted not expressed neither in CEM nor in JURKAT cells (both bearing a *PTEN* mutation), whereas it was expressed in the *PTEN* wt HPB-ALL cells. By contrast not constitutive phosphorylation of STAT5 or STAT3 was observed in CEM and Jurkat cells, with only partial pSTAT5 expression in HPB-ALL cells. Phosphoflow-based pSTATs measurement has been previously validated in our hands although in

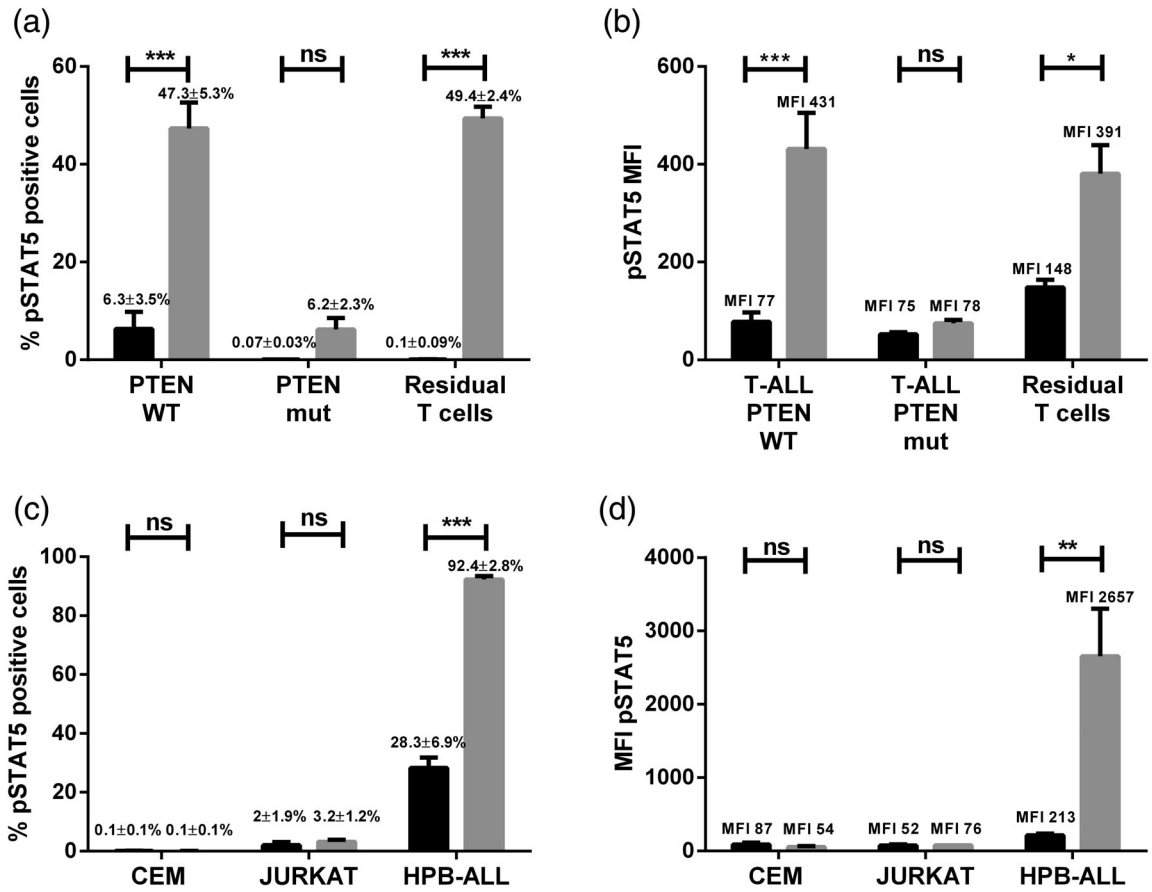

FIGURE 6 Constitutive and IL7 inducible PI3K/Akt and JAK/STAT5 pathways. (a,b) At basal state (black bars), STAT5 was not phosphorylated in T-ALL samples regardless of *PTEN* status with the exception of three PTEN wt patients (UPN 15, UPN 17, and UPN 24) due to their genetic mutation. When IL7 stimulated (gray bars), all of 16 T-ALL*PTEN* wt samples increased STAT5 phosphorylation significantly. By contrast, *PTEN* mutated patients were low or nonresponsive. These trends are consistent as both percentages and as MFI values. IL7 inducible pSTAT5 signaling in residual normal T cells was considered as positive control of functional IL7 driven pSTAT5 signaling. (c,d) T-ALL cell lines CEM and Jurkat (both *PTEN* mutated) and HPB-ALL*PTEN* wt cell lines provided similar pSTAT5 responses in term of percentages and MFI values as per the primary counterparts

different cellular subsets (Cazzaniga et al., 2015; Hasegawa et al., 2013).

We then determined the activation status of p4EBP1, PTEN, pAkt S473, and pS6 in primary T-ALL cells as compared to T cells from normal BM samples. Patient's samples showed higher protein levels confirming the constitutive hyperactivation of PI3K pathway in T-ALL (Silva et al., 2008). Of note, when we separated our T-ALL cohort based on *PTEN* status, we observed a higher pAkt S473 activation and a lower pS6 and 4pEBP1activation in PTEN-mutated samples as compared to the wt samples. To assess the accuracy of our phosphoflow approach in measuring modulated phosphosignaling nodes, we tested specific inhibitors and stimuli. We confirmed that NVP-BEZ235 is able to decrease not only Akt 473 phosphorylation but also some mTOR downstream targets such as p4EBP1 and pS6 in both primary T-ALL and T-ALL cell lines. These results suggest that the sensitivity of T-ALL to PI3K inhibition is determined by activation of the PI3K/Akt pathway rather than the level of PTEN expression, and confirm the utility of assessing the phosphorylation status of Akt, S6, and 4EBP1 as biomarkers for responsiveness among different leukemic subtypes (Badura et al., 2013; Chiarini et al., 2010; Dieterlen et al., 2012; Lynch et al., 2016; Maira et al., 2008; Silva et al., 2008).

We next investigated the JAK/STAT5 pathway by measuring basal and IL7-induced pSTAT5 levels. We showed that T-ALL blasts were not constitutively activated, with the exception of three patients (two carrying translocations involving *ABL1* gene and one with *IL7Rα* [Exon6] mutation) and the HPB-ALL cell line, which expresses endogenous pSTAT5. Intriguingly, we observed IL7-induced strong pSTAT5 responsiveness only in *PTEN* exon 7 wt blasts (11 out of 11 T-ALL primary samples), whereas mutated blasts were highly refractory to IL7 action. Similarly, HPB-ALL *PTEN* wt cells were highly pSTAT5-responsive to IL7, while *PTEN* exon 7 deleted/mutated cells lines were completely nonresponsive. Liu et al. (2017) performed an integrated genomic analysis in childhood and young adult T-ALL to characterize the spectrum and constellations of genetic alterations in this disease. They identified 10 recurrently altered pathways (Liu et al., 2017). For example, they found that JAK3/STAT5B mutations are exclusively segregated in HOX11 deregulated ALL while PIK3R1/PTEN mutations are in TAL1 ALL, suggesting that different signaling pathways have distinct roles

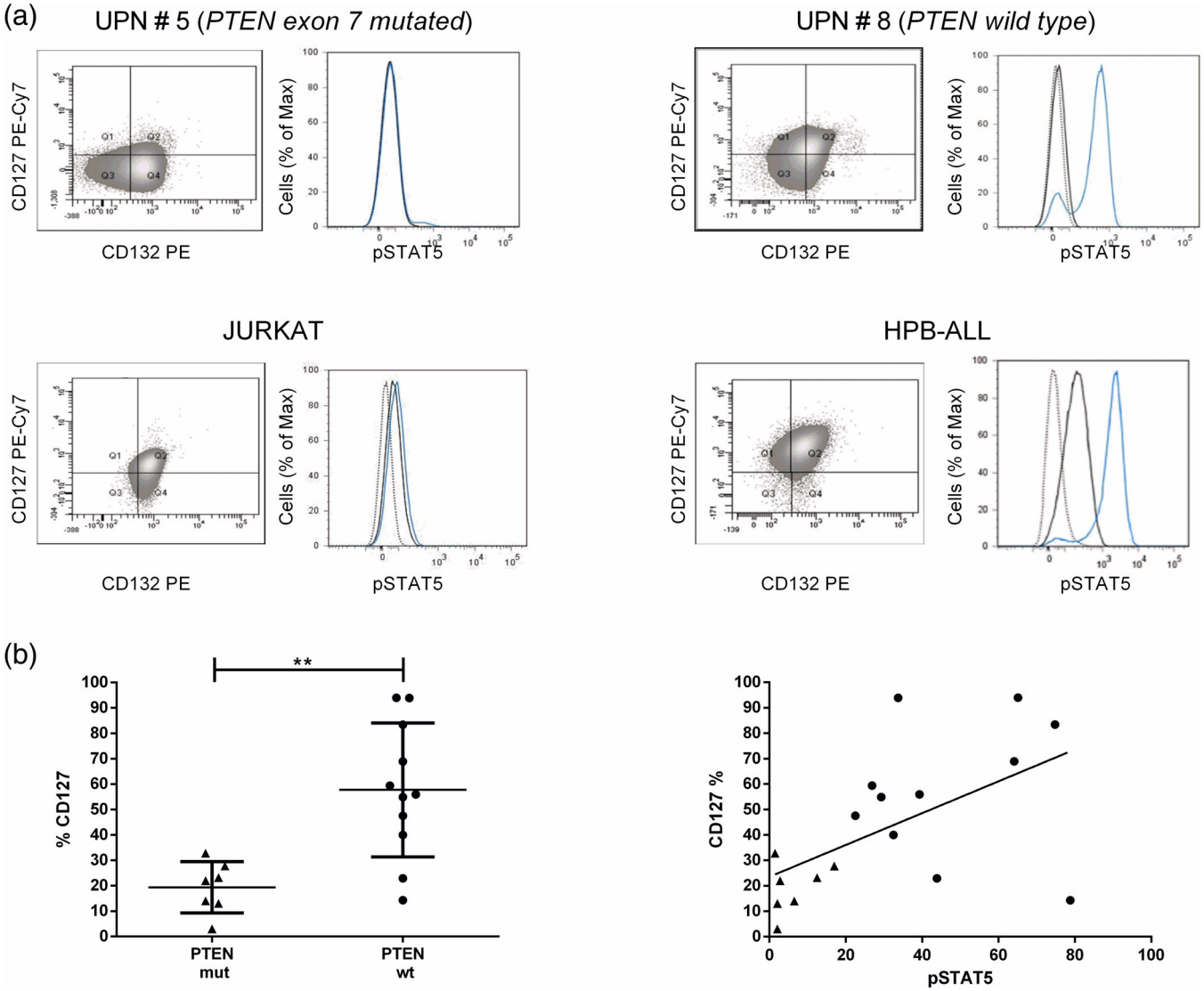

FIGURE 7 Immunophenotypic expression of the IL7 receptor according to PTEN status and correlation with IL7-induced STAT5 phosphorylation. (a) Representative dual plots of CD127/CD132 phenotypic expression and related histogram of pSTAT5 expression upon IL7 stimulation in representative *PTEN* exon 7 mutated and wt patients, in Jurkat and HPB-ALL cell lines. In histograms, blue line represents IL7-induced pSTAT5 expression, dashed line represents Isotype negative control, gray continuous line represents the basal expression, and the blue line represents the IL7-driven expression). (b) Percentage expression of surface CD127 in 18 primary T-ALL samples and linear correlation between response to IL7 stimulation and IL7 receptor expression. Pearson coefficient (p) has indicated a moderately positive correlation between the two variables ($p = .56$). *PTEN* exon 7 wt and mutated patients are indicated by circles and triangles, respectively [Color figure can be viewed at wileyonlinelibrary.com]

according to maturational stage. However, around 20% of cases had multiple signaling mutations (i.e., JAK–STAT activating mutation and concomitant PI3K-AKTmutations) raising the question of existing multi-clones and/or subclones. In our study, only two out of seven *PTEN* exon 7 mutated T-ALL were TAL1 mutated and also the maturation stage did not segregate significantly among the two subgroups (Supplemental Table S1). Although it was performed in a limited series of patients, our study here demonstrated that *PTEN* exon 7 T-ALL cases are distinctly responsive to IL7 in vitro corroborating genetic landscape data (Liu et al., 2017).

Bornschein et al. (2018) studied the association between TAL1 expression and *PTEN* deletion (Clappier et al., 2011; Mendes et al., 2014; Vicente et al., 2015). In their ex vivo pro-T cell culture model, these authors showed that both TAL1+ pro-T cells and TAL1+ T-ALL cells were unable to induce STAT5 phosphorylation in vitro upon IL7 stimulation. They found that *PTEN*-deleted/TAL1+ pro-T cells could grow in the absence of IL7, in contrast to *PTEN*-deleted alone cells.

We then investigated the correlation between IL7-driven pSTAT5 response and the expression of CD127 surface molecule in 18 T-ALL samples according to *PTEN* status. Although the expression of CD127 was significantly higher in *PTEN* wt versus *PTEN*-mutated samples, pSTAT5 response resulted only partially dependent on the amount of IL7 receptor. Furthermore, *PTEN* exon 7 mutated Jurkat cell line with

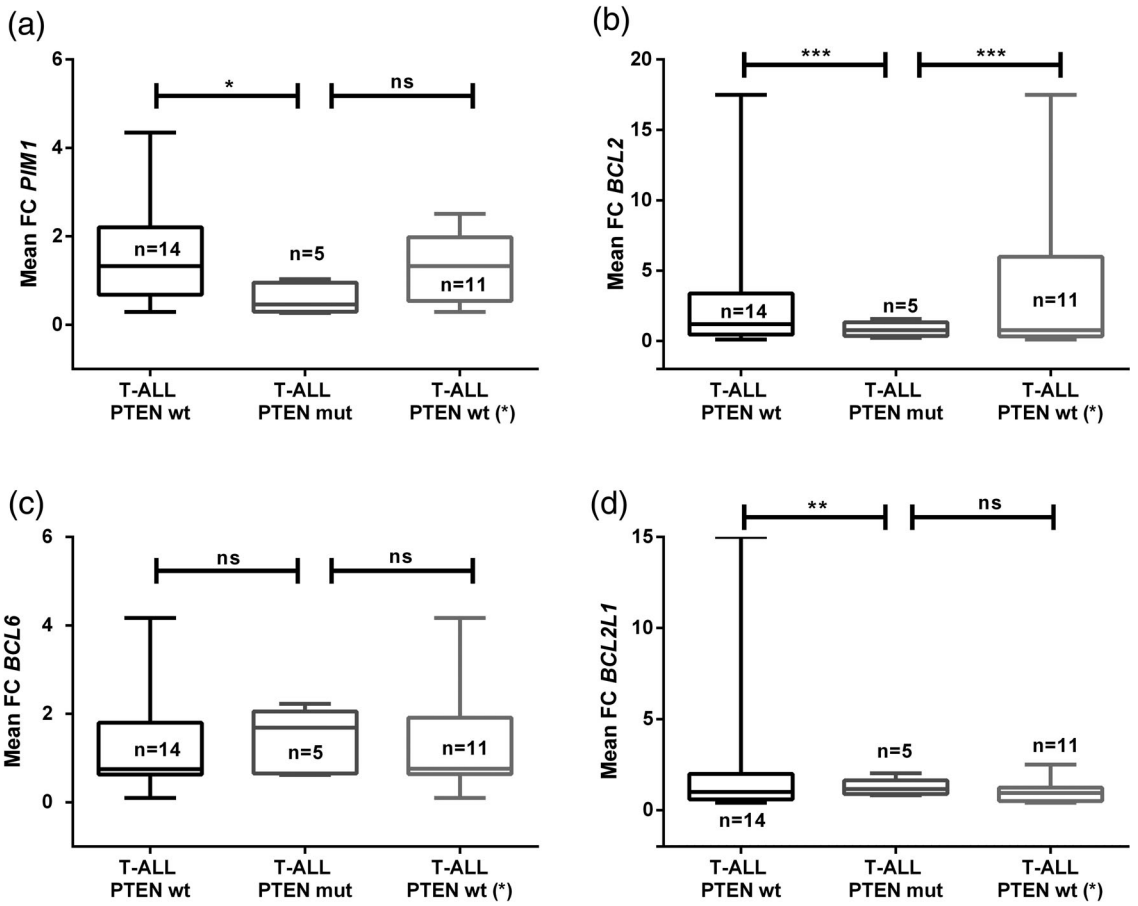

FIGURE 8 RT-qPCR analysis of gene transcript levels in T-ALL patients. (a) Box plot representation of *PIM1* transcript level in *PTEN* exon 7 mutated (n = 5) and *PTEN* exon 7 wt T-ALL with (n = 14) or (*) without pSTAT5 basically overexpressed patients (n = 11). The difference between the two subgroups became nonstatistically significant despite the difference in Fold Change means (1.293 vs. 0.588, respectively; $p > .05$). (b) *BCL2* different expression between PTEN mutated and PTEN wt T-ALL cases was confirmed despite the exclusion of pSTAT5 basically overexpressed patients ($p = .0005$) (*). (c) *BCL6* expression was nonstatistically significant between the T-ALL subgroups: one with PTEN mutation, one with PTEN wt ($p > .05$), and (*) one with PTEN wt excluding those with pSTAT5 overexpressed. (d) Box plot representation of *BCL2L1* expression in T-ALL cases. We observed that the different expression was statistically significant comparing PTEN mutated versus PTEN wt T-ALL ($p = .001$). When we excluded (*) those patients with pSTAT5 basically overexpressed (due to alterations in IL7Rα Exon6 or other rearrangements such as NUP214/ABL1 or ETV6/ABL), this expression difference became nonstatistically significant

high expression of IL7R molecules was completely nonresponsive to IL7. Recently, Ribeiro et al. (2018) demonstrated that signaling via STAT5 is mandatory for IL7-mediated survival, proliferation, and growth of T-ALL cells and it is required for increasing cell viability and cell cycle progression induced by IL7. However, IL7-mediated upregulation of *BCL2* in T-ALL is independent of STAT5 activity. Thus, we investigated *BCL2* expression in *PTEN* exon 7 wt and mutated patients, respectively, and we observed a *BCL2* downregulation in *PTEN* exon 7 mutated T-ALLs confirming findings reported by Ribeiro et al. Another IL7 and STAT5 target is PIM1, which can be upregulated by both IL7 and STAT5. We then could speculate that an alternative IL7/IL7R signaling responsible for the leukemogenic activity could be active in *PTEN* exon 7 mutated T-ALL patients (Oliveira, Akkapeddi, Ribeiro, Melao, & Barata, 2019).

In summary, we demonstrated that phosphoflow analysis represents a fast, reliable, and accurate approach to assess the signaling profiling of T-ALL, including in vitro testing of either traditional drugs or novel small molecule inhibitors over the traditional biochemical methods such as WB (Evangelisti, Chiarini, McCubrey, & Martelli, 2018; Hall, Reynolds, & Kang, 2016). In this context, we also validated the use of residual normal T cells as a valuable internal control.

Moreover, our results show that *PTEN*-mutated T-ALLs do not activate STAT5 and consequently they might not use this IL7R-driven pathway to promote survival and proliferation. According to this view, we found significantly lower expression of downstream gene *BCL2* in *PTEN*-mutated T-ALLs. It is possible that these cells activate PI3K/Akt signaling constitutively to a higher degree than PTEN wt as indicated by the higher level of Akt phosphorylation. However, further investigations are necessary to elucidate the significance of this peculiar signaling profile of *PTEN*-mutated T-ALL. We believe that our observations should be taken into account in future studies aiming at

molecular targeting of PI3K and/or JAK/STAT pathways for pharmacological intervention in T-ALL.

ACKNOWLEDGMENTS

This work was supported by Fondazione Alessandro Maria Zancan ONLUS "GrandeAle ONLUS" and Fondazione M. Tettamanti De Marchi and it was partially funded by the following grants: Italian Association for Cancer Research (AIRC IG 2017 and AIRC 5x1000 Ref. 21147 to AB), TRANSCAN-2 Fondazione Regionale per la Ricerca Biomedica (to A. B.). We also would like to thank the AIEOP centers for their support and IBISCUS onlus (No profit Association for Research and Treatment of Childhood Cancer), Catania. L. L. N. is supported by AIRC Grant (MFAG-2009).

CONFLICT OF INTEREST

The authors declare no potential conflict of interest.

ORCID

Cristina Bugarin https://orcid.org/0000-0002-7401-7097
Luca Lo Nigro https://orcid.org/0000-0002-2480-1799

REFERENCES

Abraham, N., Ma, M. C., Snow, J. W., Miners, M. J., Herndier, B. G., & Goldsmith, M. A. (2005). Haploinsufficiency identifies STATS as a modifier of IL-7-induced lymphomas. *Oncogene*, *24*, 5252–5257.

Badura, S., Tesanovic, T., Pfeifer, H., Wystub, S., Nijmeijer, B. A., Liebermann, M., … Ottmann, O. G. (2013). Differential effects of selective inhibitors targeting the PI3K/AKT/mTOR pathway in acute lymphoblastic leukemia. *PLoS One*, *8*, e80070.

Barata, J. T., Cardoso, A. A., & Boussiotis, V. A. (2005). Interleukin-7 in T-cell acute lymphoblastic leukemia: An extrinsic factor supporting leukemogenesis? *Leukemia and Lymphoma*, *46*, 483–495.

Barata, J. T., Silva, A., Brandao, J. G., Nadler, L. M., Cardoso, A. A., & Boussiotis, V. A. (2004). Activation of PI3K is indispensable for interleukin 7-mediated viability, proliferation, glucose use, and growth of T cell acute lymphoblastic leukemia cells. *The Journal of Experimental Medicine*, *200*, 659–669.

Belver, L., & Ferrando, A. (2016). The genetics and mechanisms of T cell acute lymphoblastic leukaemia. *Nature Reviews. Cancer*, *16*, 494–507.

Bongiovanni, D., Saccomani, V., & Piovan, E. (2017). Aberrant signaling pathways in T-cell acute lymphoblastic leukemia. *International Journal of Molecular Sciences*, *18*, 1–29.

Bornschein, S., Demeyer, S., Stirparo, R., Gielen, O., Vicente, C., Geerdens, E., … De Bock, C. E. (2018). Defining the molecular basis of oncogenic cooperation between TAL1 expression and Pten deletion in T-ALL using a novel pro-T-cell model system. *Leukemia*, *32*, 941–951.

Carrette, F., & Surh, C. D. (2012). IL-7 signaling and CD127 receptor regulation in the control of T cell homeostasis. *Seminars in Immunology*, *24*, 209–217.

Cazzaniga, V., Bugarin, C., Bardini, M., Giordan, M., te Kronnie, G., Basso, G., … Cazzaniga, G. (2015). LCK over-expression drives STAT5 oncogenic signaling in PAX5 translocated BCP-ALL patients. *Oncotarget*, *6*, 1569–1581.

Chiarini, F., Grimaldi, C., Ricci, F., Tazzari, P. L., Evangelisti, C., Ognibene, A., … Martelli, A. M. (2010). Activity of the novel dual phosphatidylinositol 3-kinase/mammalian target of rapamycin inhibitor NVP-BEZ235 against T-cell acute lymphoblastic leukemia. *Cancer Research*, *70*, 8097–8107.

Chow, L. M. L., & Baker, S. J. (2006). PTEN function in normal and neoplastic growth. *Cancer Letters*, *241*, 184–196.

Clappier, E., Gerby, B., Sigaux, F., Delord, M., Touzri, F., Hernandez, L., … Soulier, J. (2011). Clonal selection in xenografted human T cell acute lymphoblastic leukemia recapitulates gain of malignancy at relapse. *The Journal of Experimental Medicine*, *208*, 653–661.

Dibirdik, I., Langlie, M. C., Ledbetter, J. A., Tuel-Ahlgren, L., Obuz, V., Waddick, K. G., … Uckun, F. M. (1991). Engagement of interleukin-7 receptor stimulates tyrosine phosphorylation, phosphoinositide turnover, and clonal proliferation of human T-lineage acute lymphoblastic leukemia cells. *Blood*, *78*, 564–570.

Dieterlen, M.-T., Bittner, H. B., Klein, S., von Salisch, S., Mittag, A., Tarnok, A., … Barten, M. J. (2012). Assay validation of phosphorylated S6 ribosomal protein for a pharmacodynamic monitoring of mTOR-inhibitors in peripheral human blood. *Cytometry. Part B, Clinical Cytometry*, *82*, 151–157.

Evangelisti, C., Chiarini, F., McCubrey, J. A., & Martelli, A. M. (2018). Therapeutic targeting of mTOR in T-cell acute lymphoblastic leukemia: An update. *International Journal of Molecular Sciences*, *19*, E1878. https://doi.org/10.3390/ijms19071878

Gaipa, G., Bugarin, C., Longoni, D., Cesana, S., Molteni, C., Faini, A., … Biondi, A. (2009). Aberrant GM-CSF signal transduction pathway in juvenile myelomonocytic leukemia assayed by flow cytometric intracellular STAT5 phosphorylation measurement. *Leukemia*, *23*, 791–793.

Georgescu, M. M., Kirsch, K. H., Akagi, T., Shishido, T., & Hanafusa, H. (1999). The tumor-suppressor activity of PTEN is regulated by its carboxyl-terminal region. *Proceedings of the National Academy of Sciences of the United States of America*, *96*, 10182–10187.

Girardi, T., Vicente, C., Cools, J., & De Keersmaecker, K. (2017). The genetics and molecular biology of T-ALL. *Blood*, *129*, 1113–1123.

Gusscott, S., Jenkins, C. E., Lam, S. H., Giambra, V., Pollak, M., & Weng, A. P. (2016). IGF1R derived PI3K/AKT signaling maintains growth in a subset of human T-cell acute lymphoblastic leukemias. *PLoS One*, *11*, e0161158.

Gutierrez, A., Sanda, T., Grebliunaite, R., Carracedo, A., Salmena, L., Ahn, Y., … Look, A. T. (2009). High frequency of PTEN, PI3K, and AKT abnormalities in T-cell acute lymphoblastic leukemia. *Blood*, *114*, 647–650.

Hall, C. P., Reynolds, C. P., & Kang, M. H. (2016). Modulation of glucocorticoid resistance in pediatric T-cell acute lymphoblastic leukemia by increasing BIM expression with the PI3K/mTOR inhibitor BEZ235. *Clinical Cancer Research*, *22*, 621–632.

Hasegawa, D., Bugarin, C., Giordan, M., Bresolin, S., Longoni, D., Micalizzi, C., … Gaipa, G. (2013). Validation of flow cytometric phospho-STAT5 as a diagnostic tool for juvenile myelomonocytic leukemia. *Blood Cancer Journal*, *3*, e160.

Hunger, S. P., & Mullighan, C. G. (2015). Acute lymphoblastic leukemia in children. *The New England Journal of Medicine*, *373*, 1541–1552.

Jenkinson, S., Kirkwood, A. A., Goulden, N., Vora, A., Linch, D. C., & Gale, R. E. (2016). Impact of PTEN abnormalities on outcome in pediatric patients with T-cell acute lymphoblastic leukemia treated on the MRC UKALL2003 trial. *Leukemia*, *30*, 39–47.

Jiang, Q., Li, W. Q., Aiello, F. B., Mazzucchelli, R., Asefa, B., Khaled, A. R., & Durum, S. K. (2005). Cell biology of IL-7, a key lymphotrophin. *Cytokine & Growth Factor Reviews*, *16*, 513–533.

Johnson, S. E., Shah, N., Bajer, A. A., & LeBien, T. W. (2008). IL-7 activates the phosphatidylinositol 3-kinase/AKT pathway in normal human thymocytes but not Normal human B cell precursors. *Journal of Immunology*, *180*, 8109–8117.

Jotta, P. Y., Ganazza, M. A., Silva, A., Viana, M. B., da Silva, M. J., Zambaldi, L. J. G., … Yunes, J. A. (2010). Negative prognostic impact of PTEN mutation in pediatric T-cell acute lymphoblastic leukemia. *Leukemia*, *24*, 239–242.

Krutzik, P. O., Irish, J. M., Nolan, G. P., & Perez, O. D. (2004). Analysis of protein phosphorylation and cellular signaling events by flow

cytometry: Techniques and clinical applications. *Clinical Immunology*, *110*, 206–221.

Litzow, M. R., & Ferrando, A. A. (2015). How I treat T-cell acute lymphoblastic leukemia in adults. *Blood*, *126*, 833–841.

Liu, Y., Easton, J., Shao, Y., Maciaszek, J., Wang, Z., Wilkinson, M. R., … Mullighan, C. G. (2017). The genomic landscape of pediatric and young adult T-lineage acute lymphoblastic leukemia. *Nature Genetics*, *49*, 1211–1218.

Lynch, J. T., McEwen, R., Crafter, C., McDermott, U., Garnett, M. J., Barry, S. T., & Davies, B. R. (2016). Identification of differential PI3K pathway target dependencies in T-cell acute lymphoblastic leukemia through a large cancer cell panel screen. *Oncotarget*, *7*, 22128–22139.

Maira, S. M., Stauffer, F., Brueggen, J., Furet, P., Schnell, C., Fritsch, C., … García-Echeverría, C. (2008). Identification and characterization of NVP-BEZ235, a new orally available dual phosphatidylinositol 3-kinase/mammalian target of rapamycin inhibitor with potent in vivo antitumor activity. *Molecular Cancer Therapeutics*, *7*, 1851–1863.

Mendes, R. D., Cante-Barrett, K., Pieters, R., & Meijerink, J. P. P. (2016). The relevance of PTEN-AKT in relation to NOTCH1-directed treatment strategies in T-cell acute lymphoblastic leukemia. *Haematologica*, *101*, 1010–1017.

Mendes, R. D., Sarmento, L. M., Canté-Barrett, K., Zuurbier, L., Buijs-Gladdines, J. G. C. A. M., Póvoa, V., … Meijerink, J. P. P. (2014). PTEN microdeletions in T-cell acute lymphoblastic leukemia are caused by illegitimate RAG-mediated recombination events. *Blood*, *124*, 567–578.

Milella, M., Falcone, I., Conciatori, F., Cesta Incani, U., Del Curatolo, A., Inzerilli, N., … Ciuffreda, L. (2015). PTEN: Multiple functions in human malignant tumors. *Frontiers in Oncology*, *5*, 24.

Okkenhaug, K., & Vanhaesebroeck, B. (2003). PI3K in lymphocyte development, differentiation and activation. *Nature Reviews. Immunology*, *3*, 317–330.

Oliveira, M. L., Akkapeddi, P., Alcobia, I., Almeida, A. R., Cardoso, B. A., Fragoso, R., … Barata, J. T. (2017). From the outside, from within: Biological and therapeutic relevance of signal transduction in T-cell acute lymphoblastic leukemia. *Cellular Signalling*, *38*, 10–25.

Oliveira, M. L., Akkapeddi, P., Ribeiro, D., Melao, A., & Barata, J. T. (2019). IL-7R-mediated signaling in T-cell acute lymphoblastic leukemia: An update. *Advances in Biological Regulation*, *71*, 88–96.

Paganin, M., Grillo, M. F., Silvestri, D., Scapinello, G., Buldini, B., Cazzaniga, G., … Basso, G. (2018). The presence of mutated and deleted PTEN is associated with an increased risk of relapse in childhood T cell acute lymphoblastic leukaemia treated with AIEOP-BFM ALL protocols. *British Journal of Haematology*, *182*, 705–711.

Palomero, T., Sulis, M. L., Cortina, M., Real, P. J., Barnes, K., Ciofani, M., … Ferrando, A. A. (2007). Mutational loss of PTEN induces resistance to NOTCH1 inhibition in T-cell leukemia. *Nature Medicine*, *13*, 1203–1210.

Pongers-Willemse, M. J., Seriu, T., Stolz, F., D'Aniello, E., Gameiro, P., Pisa, P., … Van Dongen, J. J. M. (1999). Primers and protocols for standardized detection of minimal residual disease in acute lymphoblastic leukemia using immunoglobulin and T cell receptor gene rearrangements and TAL1 deletions as PCR targets. Report of the BIOMED-1 CONCERTED ACTION: Investigation of minimal residual disease in acute leukemia. *Leukemia*, *13*, 110–118.

Ribeiro, D., Melao, A., van Boxtel, R., Santos, C. I., Silva, A., Silva, M. C., … Barata, J. T. (2018). STAT5 is essential for IL-7-mediated viability, growth, and proliferation of T-cell acute lymphoblastic leukemia cells. *Blood Advances*, *2*, 2199–2213.

Rich, B. E., Campos-Torres, J., Tepper, R. I., Moreadith, R. W., & Leder, P. (1993). Cutaneous lymphoproliferation and lymphomas in interleukin 7 transgenic mice. *The Journal of Experimental Medicine*, *177*, 305–316.

Sakai, A., Thieblemont, C., Wellmann, A., Jaffe, E. S., & Raffeld, M. (1998). PTEN gene alterations in lymphoid neoplasms. *Blood*, *92*, 3410–3415.

Sansal, I., & Sellers, W. R. (2004). The biology and clinical relevance of the PTEN tumor suppressor pathway. *Journal of Clinical Oncology*, *22*, 2954–2963.

Shan, X., Czar, M. J., Bunnell, S. C., Liu, P., Liu, Y., Schwartzberg, P. L., & Wange, R. L. (2000). Deficiency of PTEN in Jurkat T cells causes constitutive localization of Itk to the plasma membrane and hyperresponsiveness to CD3 stimulation. *Molecular and Cellular Biology*, *20*, 6945–6957.

Silva, A., Laranjeira, A. B. A., Martins, L. R., Cardoso, B. A., Demengeot, J., Yunes, J. A., … Barata, J. T. (2011). IL-7 contributes to the progression of human T-cell acute lymphoblastic leukemias. *Cancer Research*, *71*, 4780–4789.

Silva, A., Yunes, J. A., Cardoso, B. A., Martins, L. R., Jotta, P. Y., Abecasis, M., … Barata, J. T. (2008). PTEN posttranslational inactivation and hyperactivation of the PI3K/Akt pathway sustain primary T cell leukemia viability. *The Journal of Clinical Investigation*, *118*, 3762–3774.

Tazzari, P. L., Cappellini, A., Bortul, R., Ricci, F., Billi, A. M., Tabellini, G., … Martelli, A. M. (2002). Flow cytometric detection of total and serine 473 phosphorylated Akt. *Journal of Cellular Biochemistry*, *86*, 704–715.

Vicente, C., Schwab, C., Broux, M., Geerdens, E., Degryse, S., Demeyer, S., … Cools, J. (2015). Targeted sequencing identifies associations between IL7R-JAK mutations and epigenetic modulators in T-cell acute lymphoblastic leukemia. *Haematologica*, *100*, 1301–1310.

Zuurbier, L., Petricoin, E. F., 3rd, Vuerhard, M. J., Calvert, V., Kooi, C., Buijs-Gladdines, J. G. C. A. M., … Meijerink, J. P. P. (2012). The significance of PTEN and AKT aberrations in pediatric T-cell acute lymphoblastic leukemia. *Haematologica*, *97*, 1405–1413.

SUPPORTING INFORMATION

Additional supporting information may be found online in the Supporting Information section at the end of this article.

How to cite this article: Bonaccorso P, Bugarin C, Buracchi C, et al. Single-cell profiling of pediatric T-cell acute lymphoblastic leukemia: Impact of *PTEN* exon 7 mutation on PI3K/Akt and JAK–STAT signaling pathways. *Cytometry*. 2020;1–13. https://doi.org/10.1002/cyto.b.21882